Australian Government
Department of Defence
Defence Science and
Technology Organisation

Phased Array Analysis Using a Modified Chebyshev Approach

Aris Alexopoulos

Electronic Warfare and Radar Division
Defence Science and Technology Organisation

DSTO–TR–1806

ABSTRACT

This report studies the antenna synthesis characteristics of linear phased arrays for both the *broadside* and *endfire* cases. The underlying technique is based on a modification of the conventional Dolph-Chebyshev side lobe tapering technique. Some of the parameters that are paramount in the design of these arrays are analysed, such as the number of elements N, the phase factor, side lobe levels, directivity, radiation pattern, element separation and impact upon SNR. The results are compared and the optimised configuration is investigated for each case.

Published by

Defence Science and Technology Organisation
PO Box 1500
Edinburgh, South Australia 5111, Australia

Telephone: *(08) 8259 5555*
Facsimile: *(08) 8259 6567*

AR No. AR-013-548
November, 2005

APPROVED FOR PUBLIC RELEASE

Phased Array Analysis Using a Modified Chebyshev Approach

EXECUTIVE SUMMARY

The work presented in this report is partially aimed towards the Microwave Radar Branch's MIcrowave RAdar Test Environment (MIRATE) project which has the objectives of allowing microwave radar researchers and engineers to build skills and first hand knowledge of phased array radars and to generally foster R & D that ultimately will be used for the analysis of more complex phased array radar systems such as the one anticipated to go into the new Air Warfare Destroyer (Project SEA 4000). Specifically, one component under MIRATE is the construction of an operational experimental phased array radar (XPAR), which as a first step, comprises the development of a 16-element linear array. This report presents theoretical results that can be tested experimentally by the XPAR program and it is hoped that other methods and techniques will be studied and implemented throughout various stages of XPAR.

The approach here is to consider an arbitrary number of linear arrays and study the various design specifications that might surface for such a system using a method based on conventional Dolph-Chebyshev tapering techniques. By using a modified Chebyshev approach (MC) we investigate amongst other things the side lobe level, directivity, radiation pattern, element spacing, relation to the number of elements and so on. The MC method has superior convergence properties for large arrays given that the window coefficients of the radiation pattern can be determined via the use of matrix algebra. At the same time this avoids the use of complicated polynomial equations that are computationally intense. Results presented are for both *broadside* and *endfire* arrays and comparison shows interesting behaviour depending on the selection of either an even or odd number of elements.

Author

Aris Alexopoulos
Electronic Warfare and Radar Division

Aris Alexopoulos is a theoretical physicist and holds a First Class BSc(Honours) degree as well as a PhD degree. His research interests are in the areas of nanotechnology, radar systems, electromagnetic propagation and non-linear/fractal electrodynamics.

Contents

1 Introduction **1**

2 The Array Factor **1**

2.1 The Excitation Amplitudes 3

3 The Power Aperture Product of a Weighted Array **12**

4 The Impact on the Signal to Noise Ratio of a Weighted Array **13**

5 Investigation of Beamwidth, Side Lobe Level and the Number of Elements **18**

6 Optimising the Inter-Element Separation **20**

7 Directivity **20**

8 Conclusion **25**

References **26**

Figures

1 Linear array with elements radiating at angle θ and phase-shift α. The inter-element separation is d. 2

2 (i) For an even number of elements N, the amplitude distributions are obtained by normalising all other amplitudes by the edge element a_n. The calculations in Tables 1-2 refer to this configuration for even N, where the symmetry point is taken to be at a distance of $d/2$ from the element with amplitude a_1. (ii) the same as before except we now consider an odd number of elements N with the symmetry occuring at the element with amplitude a_0 at a distance of d from a_1. 3

3 **Left Plot**: The array factor as a function of u for $|SLL| = -10$ dB. The curve in red represents $N = 17$ (odd) number of elements while the curve in blue is for $N = 20$ (even). **Right Plot**: Polar plot for the parameters used on the left. 9

4 **Left Plot**: The array factor as a function of u for $|SLL| = -10$ dB. The curve in red represents $N = 11$ (odd) number of elements while the curve in blue is for $N = 10$ (even). **Right Plot**: Polar plot for the parameters used on the left. 9

5 **Left Plot**: The array factor as a function of u for $|SLL| = -13$ dB. The curve in red represents $N = 17$ (odd) number of elements while the curve in blue is for $N = 20$ (even). **Right Plot**: Polar plot for the parameters used on the left. 9

6 The solid curve is obtained from (38), while the points represent the number of elements N for each average power $< a >$. 11

7 **Left Plot**: The total transmitted aperture power is shown vs a relatively small number of array elements N at different sidelobe levels. **Right Plot**: The efficiency of the aperture power of arrays is shown vs the number of elements. 13

8 **Left Plot**: The total transmitted aperture power is shown vs $N = 100$ array elements at different sidelobe levels. **Right Plot**: The efficiency of the aperture power of the arrays is shown vs the number of elements. 14

9 **Left Plot**: The total transmitted aperture power is shown vs a relatively large number of array elements at different sidelobe levels. **Right Plot**: The efficiency of the aperture power of the arrays is shown vs the number of elements. 14

10 **Left Plot**: The total transmitted aperture power is shown vs the number of elements at different sidelobe levels for a two-way transmit and receive SLL. Comparison is made of the power for an unweighted transmition but weighted reception of SLL=-40 dB to that of a transmit and receive mode of SLL=-20 dB. **Right Plot**: The efficiency of the aperture power of the arrays is shown vs the number of elements. 15

11 Impact upon SNR of Chebyshev weights applied on reception only. 16

12 Impact upon SNR of Chebyshev weights applied both on transmit and reception. 17

13 Impact upon SNR of Chebyshev weights applied on transmit and reception compared with reception only. 17

14 The optimised spacing plotted against the number of elements for an X-Band ($\lambda = 0.03$ m) array. The curves starting from the bottom to the top correspond to $|SLL| = -10, -20, -30$ and -40 dB's respectively. 18

15 The optimised spacing plotted against the number of elements for an L-Band ($\lambda = 0.25$ m) array on the left and an S-Band ($\lambda = 0.1$ m) array on the right. The curves starting from the bottom to the top correspond to $|SLL| = -10, -20, -30$ and -40 dB's respectively. 19

16 Comparison of the half-power beamwidth ($HPBW$) for a broadside array (left) and an end-fire array (right) with optimum spacing between the elements. The dashed curve's side lobe ratio is -10 dB, while the solid curve is that for a -40 dB side lobe ratio. 21

17 The half-power beamwidth ($HPBW$) in degrees plotted against the number of elements for a broadside array (left) and an end-fire array (right). The dashed curve represents an array spacing of $\lambda/2$ while the solid curve is the optimised spacing. The magnitude of the side lobe level is -10 dB. 22

18 The half-power beamwidth ($HPBW$) in degrees plotted against the number of elements for a broadside array (left) and an end-fire array (right). The dashed curve represents an array spacing of $\lambda/2$ while the solid curve is the optimised spacing. The magnitude of the side lobe level is -20 dB. 22

19 The half-power beamwidth ($HPBW$) in degrees plotted against the number of elements for a broadside array (left) and an end-fire array (right). The dashed curve represents an array spacing of $\lambda/2$ while the solid curve is the optimised spacing. The magnitude of the side lobe level is -30 dB. 22

20 The half-power beamwidth ($HPBW$) in degrees plotted against the number of elements for a broadside array (left) and an end-fire array (right). The dashed curve represents an array spacing of $\lambda/2$ while the solid curve is the optimised spacing. The magnitude of the side lobe level is -40 dB. 23

21 The relation between the SLL, the ratio of the optimum spacing to the wavelength (d_{opt}/λ) and the number of elements N. The plot on the left is for a **broadside** array while the plot on the right is for an **end − fire** array. 24

22 Plots of the directivity D against the ratio d/λ for a broadside array (the end-fire case differs by a factor of 1/2). The number of elements that have been chosen are $N = 3, 7, 12, 16, 19$ and 20, where $N = 3$ is the lowest curve and $N = 20$ is the highest in each plot. The side lobe level is: **-10 dB for the left plot and -20 dB for the right plot**. 24

23 Plots of the directivity D against the ratio d/λ for a broadside array (the end-fire case differs by a factor of 1/2). The number of elements that have been chosen are $N = 3, 7, 12, 16, 19$ and 20, where $N = 3$ is the lowest curve and $N = 20$ is the highest in each plot. The side lobe level is: **-30 dB for the left plot and -40 dB for the right plot**. 25

Tables

1 Amplitude magnitudes for equally spaced Modified Chebyshev arrays. Note that the amplitudes of the edge elements are always unity and all other amplitudes are normalised by the former, see Figure 2. The Table below shows values such that the first row corresponds to a_1 (even) or a_0 (odd), the second row corresponds to a_2,...., a_{n-1}, $a_n = 1$. 4

2 Continued from Table 1. Amplitude magnitudes for equally spaced Modified Chebyshev arrays. Note that the amplitudes of the edge elements are always unity and all other amplitudes are normalised by the former, see Figure 2. The Table below shows values such that the first row corresponds to a_1 (even) or a_0 (odd), the second row corresponds to a_2,...., a_{n-1}, $a_n = 1$. 5

3 Polynomial approximation for the $HPBW$ using the optimum spacing between the radiating elements N for a **broadside** array. The left hand column represents the side lobe ratio, while the right side column is the approximation to the half-power beamwidth in degrees for any $N = 3, ..., 20$. 10

4 Polynomial approximation for the $HPBW$ using the optimum spacing between the radiating elements N for an **end − fire** array. The left hand column represents the side lobe ratio, while the right side column is the approximation to the half-power beamwidth in degrees for any $N = 3, ..., 20$. 11

1 Introduction

In this report we will consider an analysis that involves a variation of the technique used in conventional Chebyshev arrays. A key aspect of Chebyshev arrays is that they produce equal side lobe levels (SLL) for a given radiation pattern. However, Chebyshev arrays suffer from directivity saturation when the number of radiating elements becomes large [1]. Thus there is a need to find a method to analyse large Chebyshev arrays in an efficient manner. Furthermore, the synthesis of the radiation pattern is difficult because for every radiation pattern a new complicated polynomial series needs to be found. It is of no surprise that researchers have been looking for alternatives in order to overcome these inefficiencies [2]. What we shall call the Modified Chebyshev (MC) method, is a technique that is based on the synthesis of arrays using the zeros of conventional Chebyshev arrays repeatedly, see for example [3]. More specifically, the idea behind the MC formulation is that it makes no direct use of Chebyshev polynomials. The array factor is calculated in terms of cosine and hyperbolic cosine functions respectively, while a system of equations for the excitation amplitudes is obtained from the zeros of the array factor. The solution of the system of equations for the excitation amplitudes is done by allowing one of those excitation amplitudes to be the independent variable, as we shall see later. The procedure allows for the solution of any number of radiating elements N, for both an even or odd configuration of arrays respectively. Lee [4] has used the zeros of the array factor before in order to study a different formulation of Chebyshev arrays, however the method still uses a polynomial representation for the array factor, which does not generalise and becomes mathematically involved when we consider a large number of elements or large arrays. The problem of beam synthesis for example, involving an unknown number of elements but specified SLL and beamwidth, is tackled traditionally by determining the minimum number of elements that are required to meet the design parameters through a trial and error process. In what follows, we will examine a process that allows the minimum number of elements to be obtained in a single step without resorting to an iterative process, hence giving a more flexible and efficient design strategy. Furthermore we assume that among the SLL, half-power beamwidth, and number of elements, two quantities are specified and the third quantity as well as the excitation amplitudes [1] are sought. In addition, we will also consider both broadside and endfire arrays as well as the optimum spacing between the radiating elements.

2 The Array Factor

We consider a linear array of N equally spaced elements with uniform excitations and symmetrical distributions for the magnitude amplitudes in the array, as well as a constant inter-element phase shift α of radiating electromagnetic waves at angle θ from the plane of the array-refer to Figure 1. For an even and odd number of elements we can express the array factor as,

[1] These are obtained relative to the amplitude of one element that is taken as the independent variable

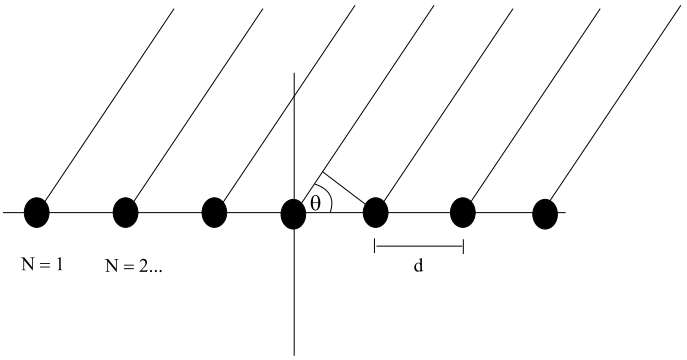

Figure 1: *Linear array with elements radiating at angle θ and phase-shift α. The inter-element separation is d.*

$$f(\psi) = 2\sum_{m=1}^{n} a_m \cos\left[\left(m - \tfrac{1}{2}\right)\psi\right] \quad ; N = 2n, \tag{1}$$

and

$$f(\psi) = a_0 + 2\sum_{m=1}^{n} a_m \cos\left[m\psi\right] \quad ; \; N = 2n+1, \tag{2}$$

where $\psi = \beta d\cos(\theta) + \alpha$, $\beta = 2\pi/\lambda$; λ is the wavelength, d is the element spacing, α is the phase factor, θ is the angle measured from the line of the array, a_m is the magnitude of the amplitude for the m^{th} element on either side of the array midpoint and a_0 denotes the amplitude of the centre element when N is odd. Given the fact that Chebyshev polynomials satisfy the relationships $T_n(\cos x) = \cos(nx)$ for $|T_n| < 1$ and $T_n\cos(hx) = \cosh(nx)$ for $T_n \geq 1$, the array factor in (1) or (2) is written as

$$|f(\psi)| = |f(\bar{\psi})| = \begin{cases} C\left|\cos\left[\left(\frac{(N-1)}{2}\bar{\psi}\right)\right]\right| & ; \; |f(\psi)| \leq C \\ C\cosh\left[\left(\frac{(N-1)}{2}\bar{\psi}\right)\right] & ; \; |f(\psi)| \geq C, \end{cases} \tag{3}$$

where C is a positive constant coefficient and ψ is related to $\bar{\psi}$ by

$$\gamma\cos\left(\tfrac{\psi}{2}\right) = \begin{cases} \cos\left(\frac{\bar{\psi}}{2}\right) & ; \; |f(\psi)| \leq C \\ \cosh\left(\frac{\bar{\psi}}{2}\right) & ; \; |f(\psi)| \geq C. \end{cases} \tag{4}$$

In (4) we note that γ is a real coefficient that can be determined when the design specifications are considered. By close examination of (3), we find that $f(\psi)$ assumes its maximum value when $\bar{\psi} = 0$. Moreover, this corresponds to $\bar{\psi} \equiv \bar{\psi}_0 = 2\cosh^{-1}(\gamma)$. In most cases of interest, we can assume a knowledge of the number of radiating elements N and the maximum-to-side lobe level ratio R [2] . Since we assume that the side lobes have the same magnitude (see (3)), we can write down the ratio R as

$$R = \cosh\left[\left(\frac{(N-1)}{2}\bar{\psi}_0\right)\right] = \cosh\left[(N-1)\cosh^{-1}(\gamma)\right]. \tag{5}$$

By transposing (5) and solving for γ we obtain:

$$\gamma = \cosh\left[\frac{1}{(N-1)}\log_e(R + \sqrt{R^2-1})\right]. \tag{6}$$

[2]The side lobe level here is: $-20log_{10}(R)$ in dB.

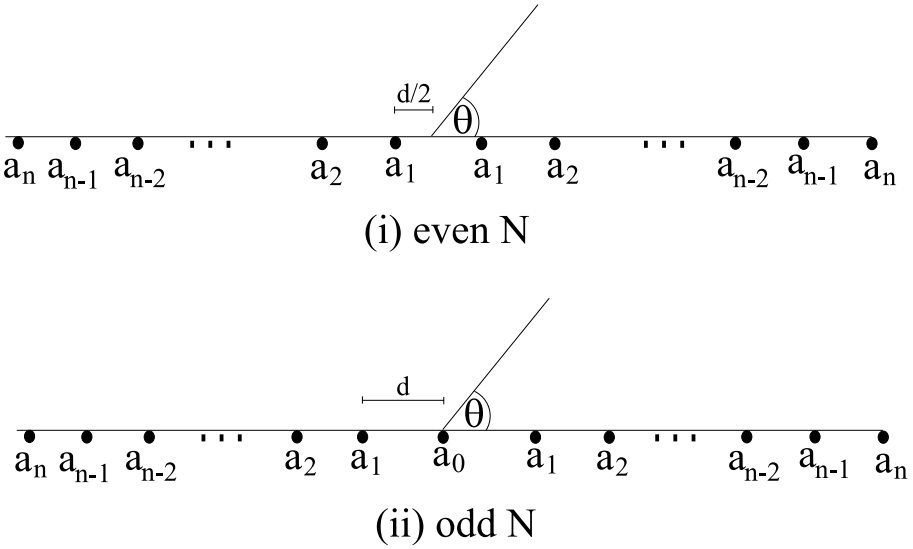

Figure 2: *(i) For an even number of elements N, the amplitude distributions are obtained by normalising all other amplitudes by the edge element a_n. The calculations in Tables 1-2 refer to this configuration for even N, where the symmetry point is taken to be at a distance of $d/2$ from the element with amplitude a_1. (ii) the same as before except we now consider an odd number of elements N with the symmetry occuring at the element with amplitude a_0 at a distance of d from a_1.*

We are now in a position to calculate γ when we know N and the half-power beamwidth HPBW or alternatively we can do the same if we know R and the HPBW as we shall see later. Finally, if we require the array factor to be normalised to unity, we can determine the coefficient $C = 1/R$.

2.1 The Excitation Amplitudes

A system of equations that govern the magnitude of the radiating elements can be constructed from the zeros of the array factor in terms of matrices. These zeros are solutions of $\cos[(N-1)\bar{\psi}/2] = 0$, and when rearranging for $\bar{\psi}$ we obtain the solutions $\bar{\psi} = [(4m \pm 1)\pi]/(N-1)$, with m being an integer. The fact that the array factor is symmetrical about $\bar{\psi} = \pi$ allows us to consider only the zeros in the range $0 < \bar{\psi} < \pi$-see Figure 2 for the distribution of the elements. The zeros are now obtained from,

$$\bar{\psi}_m = \frac{(2m-1)\pi}{N-1}, \tag{7}$$

for $m = 1, 2, 3, ..., M$, while $M = (N-2)/2$ for N even and $M = (N-1)/2$ for N odd number of radiating elements respectively. More explicitly we obtain the zeros in terms of ψ by

$$\psi_m = 2\cos^{-1}\left[\frac{1}{\gamma}\cos\left(\frac{(2m-1)\pi}{2(N-1)}\right)\right], \tag{8}$$

Table 1: *Amplitude magnitudes for equally spaced Modified Chebyshev arrays. Note that the amplitudes of the edge elements are always unity and all other amplitudes are normalised by the former, see Figure 2. The Table below shows values such that the first row corresponds to a_1 (even) or a_0 (odd), the second row corresponds to a_2,...., a_{n-1}, $a_n = 1$.*

N	$\|SLL\| = -10$ dB	$\|SLL\| = -20$ dB	$\|SLL\| = -30$ dB	$\|SLL\| = -40$ dB
3	1.0390	1.6364	1.8774	1.9604
	1	1	1	1
4	0.8794	1.7357	2.3309	2.6688
	1	1	1	1
5	0.7975	1.9319	3.1397	4.1448
	0.7248	1.6085	2.4123	3.0131
	1	1	1	1
6	0.6808	1.8499	3.3828	4.9891
	0.6071	1.4369	2.3129	3.0853
	1	1	1	1
7	0.6102	1.8387	3.7846	6.2731
	0.5864	1.6837	2.3071	5.2678
	0.5191	1.2764	2.1507	3.0071
	1	1	1	1
8	0.5413	1.7244	3.8136	6.8448
	0.5103	1.5091	3.0965	5.1982
	0.4519	1.1386	1.9783	2.8605
	1	1	1	1
9	0.4923	1.6627	3.9565	7.6989
	0.4813	1.5800	3.6516	6.9168
	0.4494	1.3503	2.8462	4.9516
	0.3995	1.0231	1.8158	2.6901
	1	1	1	1
10	0.4463	1.5585	3.8830	7.9837
	0.4306	1.4360	3.4095	6.6982
	0.4003	1.2125	2.5986	4.6319
	0.3576	0.9264	1.6695	2.5182
	1	1	1	1
11	0.4113	1.4907	3.8985	8.4813
	0.4054	1.4421	3.6982	7.8954
	0.3880	1.3036	3.1457	6.3341
	0.3601	1.0949	2.3702	4.2952
	0.3235	0.8450	1.5400	2.3546
	1	1	1	1
12	0.3787	1.4031	3.7865	8.5669
	0.3697	1.3277	3.4657	7.5913
	0.3521	1.1860	2.8885	5.9124
	0.3269	0.9948	2.1659	3.9692
	0.2952	0.7759	1.4262	2.2035
	1	1	1	1

Table 2: *Continued from Table 1. Amplitude magnitudes for equally spaced Modified Chebyshev arrays. Note that the amplitudes of the edge elements are always unity and all other amplitudes are normalised by the former, see Figure 2. The Table below shows values such that the first row corresponds to a_1 (even) or a_0 (odd), the second row corresponds to a_2,...., a_{n-1}, $a_n = 1$.*

N	$\|SLL\| = -10$ dB	$\|SLL\| = -20$ dB	$\|SLL\| = -30$ dB	$\|SLL\| = -40$ dB
13	0.3528	1.3408	3.7438	8.8242
	0.3492	1.3101	3.6071	8.3860
	0.3387	1.2218	3.2208	7.1776
	0.3217	1.0830	2.6498	5.4821
	0.2990	0.9093	1.9856	3.6660
	0.2713	0.7167	1.3261	2.0658
	1	1	1	1
14	0.3286	1.2683	3.6224	8.7888
	0.3229	1.2189	3.3979	8.0481
	0.3119	1.1245	2.9818	6.7204
	0.2958	0.9931	2.4335	5.0683
	0.2753	0.8358	1.8273	3.3899
	0.2510	0.6655	1.2379	1.9409
	1	1	1	1
15	0.3086	1.2138	3.5549	8.8944
	0.3064	1.1932	3.4582	8.5628
	0.2996	1.1330	3.1807	7.6287
	0.2885	1.0378	2.7574	6.2585
	0.2735	0.9146	2.2401	4.6829
	0.2549	0.7724	1.6883	3.1411
	0.2335	0.6209	1.1598	1.8281
	1	1	1	1

where $m = 1, 2, 3, ..., M$. We make the observation that the ψ_m's are zeros of $f(\psi)$ in (1) or (2), that is,

$$f(\psi_m) = 0, \quad m = 1, 2, 3, ..., M. \tag{9}$$

In fact (9) gives a system of M equations with $M + 1$ unknowns. These unknowns to be solved are the amplitudes of the radiating elements a_M, one of which is chosen as the independent variable. In the case of an even number of elements, the independent variable is chosen to be a_{M+1}. We can form matrices that allow us to solve for any number of array elements N. From (1) we have the form

$$f(\psi_k) = 2 \sum_{m=1}^{n} a_m \cos\left[\left(m - \frac{1}{2}\right)\psi_k\right], \tag{10}$$

for $k = 1, 2, 3, ..., M$. The solution of (10) for the amplitudes a_m can be calculated from the form

$$\begin{bmatrix} a_1 & a_2 & \cdots & a_M \end{bmatrix}^T = -a_{M+1} \left[\begin{bmatrix} \vec{\gamma}_1 & \vec{\gamma}_2 & \cdots & \vec{\gamma}_M \end{bmatrix}^T \right]^{-1} \times \begin{bmatrix} \cos[(M+1/2)\psi_1] & \cos[(M+1/2)\psi_2] & \cdots & \cos[(M+1/2)\psi_M] \end{bmatrix}^T , \quad (11)$$

which can be abbreviated to,

$$\vec{a}^T = -a_{M+1} \left[\vec{A}^T \right]^{-1} \vec{C}^T , \quad (12)$$

where T is the transpose. We will examine (12) and therefore define the matrices $\vec{A}$, $\vec{C}$ and the vectors $\vec{\gamma}$, by solving (10) via (12) for $k = 1, 2$. Furthermore, we will consider $N = 6$ elements for the array, and because we are dealing with an even number of elements we have $M = 2$. From this we know that the independent variable we need is given by a_{M+1} or a_3. Expanding (10) we obtain

$$f(\psi_1) = 2a_1 \cos\left(\frac{\psi_1}{2}\right) + 2a_2 \cos\left(\frac{3\psi_1}{2}\right) + 2a_3 \cos\left(\frac{5\psi_1}{2}\right), \quad (13)$$

and

$$f(\psi_2) = 2a_1 \cos\left(\frac{\psi_2}{2}\right) + 2a_2 \cos\left(\frac{3\psi_2}{2}\right) + 2a_3 \cos\left(\frac{5\psi_2}{2}\right). \quad (14)$$

Now from (9) we know that the expansions in (13) and (14) are zero, ie,

$$\begin{pmatrix} f(\psi_1) \\ f(\psi_2) \end{pmatrix} = \begin{pmatrix} 0 \\ 0 \end{pmatrix}. \quad (15)$$

Equating (13) and (14) to zero and transposing the independent amplitude and its coefficient to one side, it is easy to show that we obtain the matrices:

$$\begin{pmatrix} \cos\left(\frac{\psi_1}{2}\right) & \cos\left(\frac{3\psi_1}{2}\right) \\ \cos\left(\frac{\psi_2}{2}\right) & \cos\left(\frac{3\psi_2}{2}\right) \end{pmatrix} \begin{pmatrix} a_1 \\ \\ a_2 \end{pmatrix} = -a_3 \begin{pmatrix} \cos\left(\frac{5\psi_1}{2}\right) \\ \cos\left(\frac{5\psi_2}{2}\right) \end{pmatrix}. \quad (16)$$

We recall that a_3 in (16) is the independent variable and has been transposed to the right side. We are of course interested in solving (16) for the amplitudes and so we have

$$\begin{pmatrix} a_1 \\ \\ a_2 \end{pmatrix} = -a_3 \begin{pmatrix} \cos\left(\frac{\psi_1}{2}\right) & \cos\left(\frac{3\psi_1}{2}\right) \\ \cos\left(\frac{\psi_2}{2}\right) & \cos\left(\frac{3\psi_2}{2}\right) \end{pmatrix}^{-1} \begin{pmatrix} \cos\left(\frac{5\psi_1}{2}\right) \\ \cos\left(\frac{5\psi_2}{2}\right) \end{pmatrix}. \quad (17)$$

The solutions for a_1 and a_2 satisfy the array factor (1) or (10), for an even number of radiating elements N. If we let

$$\begin{aligned} \vec{a}^T &= \begin{bmatrix} a_1 & a_2 \end{bmatrix}^T \\ \vec{C}^T &= \begin{bmatrix} \cos\left(\frac{5\psi 1}{2}\right) & \cos\left(\frac{5\psi_2}{2}\right) \end{bmatrix}^T \\ \vec{A}^T &= \begin{bmatrix} \vec{\gamma}_1 & \vec{\gamma}_2 \end{bmatrix}^T \end{aligned} \quad (18)$$

and

$$\begin{array}{l}\vec{\gamma}_1 = \left[\begin{array}{cc} \cos\left(\frac{\psi_1}{2}\right) & \cos\left(\frac{3\psi_1}{2}\right) \end{array}\right. \\ \vec{\gamma}_2 = \left.\begin{array}{cc} \cos\left(\frac{\psi_2}{2}\right) & \cos\left(\frac{3\psi_2}{2}\right) \end{array}\right] \end{array}, \tag{19}$$

we recover (12) for the case $k = 1, 2$. The procedure we have studied so far means that we can generalise the results above to any number of radiating elements, and it is easy to extend to the general form;

$$\begin{pmatrix} a_1 \\ a_2 \\ \vdots \\ a_M \end{pmatrix} = -a_{M+1}[\vec{A}^T]^{-1} \begin{pmatrix} \cos[(M+\frac{1}{2})\psi_1] \\ \cos[(M+\frac{1}{2})\psi_2] \\ \vdots \\ \cos[(M+\frac{1}{2})\psi_M] \end{pmatrix}, \tag{20}$$

where the matrix $\vec{A}^T$ has the general form,

$$\vec{A}^T = \begin{pmatrix} \cos\left(\frac{\psi_1}{2}\right) & \cos\left(\frac{3\psi_1}{2}\right) & \cdots & \cos\left[(M+\frac{1}{2})\frac{\psi_1}{2}\right] \\ \cos\left(\frac{\psi_2}{2}\right) & \cos\left(\frac{3\psi_2}{2}\right) & \cdots & \cos\left[(M+\frac{1}{2})\frac{\psi_2}{2}\right] \\ \vdots & \vdots & & \vdots \\ \cos\left(\frac{\psi_M}{2}\right) & \cos\left(\frac{3\psi_M}{2}\right) & \cdots & \cos\left[(M+\frac{1}{2})\frac{\psi_M}{2}\right] \end{pmatrix}^T. \tag{21}$$

Here $M = (N-2)/2$ for an even number of array elements N. In a similar way we can now consider the case where N is an odd number of elements. For example, if $N = 5$, we obtain from $M = (N-1)/2$ that $M = 2$ and we also recall that the independent variable is chosen to be a_0 . The array factor (2) can be written as

$$f(\psi_k) = a_0 + 2\sum_{m=1}^{n} a_m \cos[m\psi_k], \tag{22}$$

so if we seek solutions for $k = 1$, and 2 for instance we obtain the expansions

$$f(\psi_1) = a_0 + 2a_1\cos(\psi_1) + 2a_2\cos(2\psi_1) \tag{23}$$

and

$$f(\psi_2) = a_0 + 2a_1\cos(\psi_2) + 2a_2\cos(2\psi_2). \tag{24}$$

From (15) we find once again that (23) and (24) can be written as

$$2\begin{pmatrix} \cos(\psi_1) & \cos(2\psi_1) \\ \cos(\psi_2) & \cos(2\psi_2) \end{pmatrix}\begin{pmatrix} a_1 \\ a_2 \end{pmatrix} = -\begin{pmatrix} a_0 \\ a_0 \end{pmatrix}, \tag{25}$$

which finally gives the solutions

$$\begin{pmatrix} a_1 \\ a_2 \end{pmatrix} = -\frac{1}{2}a_0\begin{pmatrix} \cos(\psi_1) & \cos(2\psi_1) \\ \cos(\psi_2) & \cos(2\psi_2) \end{pmatrix}^{-1}\begin{pmatrix} 1 \\ 1 \end{pmatrix}. \tag{26}$$

As we have done so before, we can now generalise for odd N by writing the generalised form as

$$\begin{pmatrix} a_1 \\ a_2 \\ \vdots \\ a_M \end{pmatrix} = -\frac{1}{2}a_0\left[\vec{B}\right]^{-1}\begin{pmatrix} 1 \\ 1 \\ \vdots \\ 1 \end{pmatrix}, \tag{27}$$

or in the vector-matrix form

$$\vec{a}^T = -\frac{1}{2} a_0 \left[\vec{B}^T\right]^{-1} \vec{I}, \tag{28}$$

where the matrix $\vec{B}^T$ becomes

$$\vec{B}^T = \begin{pmatrix} \cos(\psi_1) & \cos(2\psi_1) & \cdots & \cos(M\psi_1) \\ \cos(\psi_2) & \cos(2\psi_2) & \cdots & \cos(M\psi_2) \\ \vdots & \vdots & & \vdots \\ \cos(\psi_M) & \cos(2\psi_M) & \cdots & \cos(M\psi_M) \end{pmatrix}^T. \tag{29}$$

The solutions for a_m satisfy the array factor as given by (2) for an odd number of elements N. Table 1 shows the calculated amplitude coefficients for even and odd radiating elements using the technique discussed above. Also, the method investigated so far hints at the possibility of obtaining the amplitudes via a series. Indeed this is the case, such a series solution is based on the work by Barbiere [5] but for large arrays there are convergence problems. For small arrays it gives excellent results that allow comparison of the amplitudes for an even or odd number of elements. We first define the variable z_0 to be:

$$z_0 = \frac{1}{2}\left[\left(R + \sqrt{R^2-1}\right)^{\frac{1}{(M-1)}} + \left(R - \sqrt{R^2-1}\right)^{\frac{1}{(M-1)}}\right], \tag{30}$$

where R once again represents the ratio of the side lobe level. For an even number of elements, $M = N/2$, and the amplitudes are given by

$$a_n = \sum_{q=n}^{M} \frac{(2M-1)(q+M-2)!}{(q-n)!(q+n-1)!(M-q)!}(-1)^{M-q} z_0^{2q-1}. \tag{31}$$

Alternatively, for an odd number of elements $M = (N-1)/2$, and thus we obtain the amplitudes by the series expansion,

$$a_n = \sum_{q=n}^{M-1} \frac{2M(q+M-2)!}{\varepsilon_n (q-n)!(q+n-2)!(M-q+1)!}(-1)^{M-q+1} z_0^{2(q-1)}, \tag{32}$$

with the additional condition that ϵ_n is given by

$$\varepsilon_n = \begin{cases} 2, & n = 1 \\ 1, & n \neq 1 \end{cases} \tag{33}$$

such that $n = 1, 2, 3, ...$ It is now a matter of expanding the even and odd solutions of the array factors respectively,

$$AF^{(even)} = \sum_{n=1}^{M} a_n \cos\left[(2n-1)u\right] \tag{34}$$

and

$$AF^{(odd)} = \sum_{n=1}^{M+1} a_n \cos\left[(2n-1)u\right], \tag{35}$$

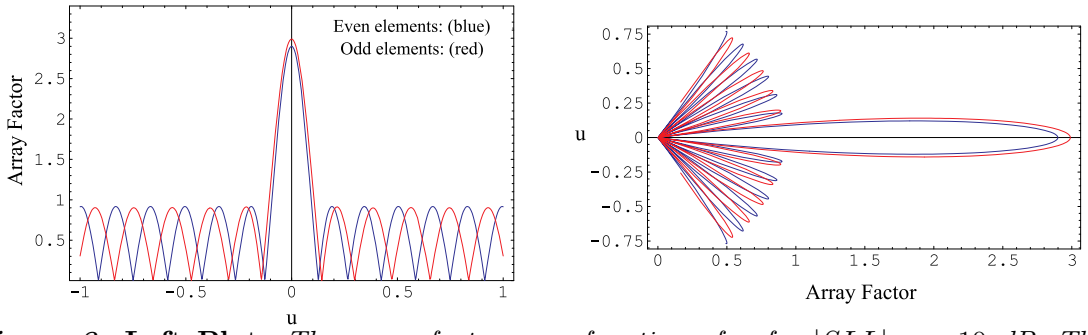

Figure 3: **Left Plot**: *The array factor as a function of* u *for* $|SLL| = -10$ *dB. The curve in red represents* $N = 17$ *(odd) number of elements while the curve in blue is for* $N = 20$ *(even).* **Right Plot**: *Polar plot for the parameters used on the left.*

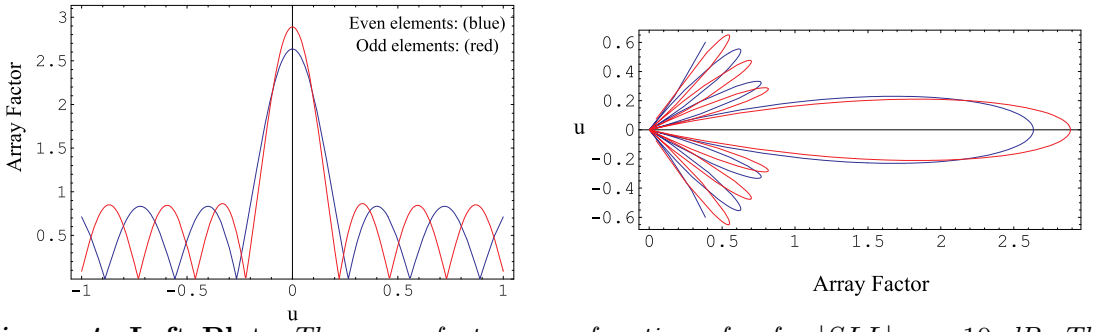

Figure 4: **Left Plot**: *The array factor as a function of* u *for* $|SLL| = -10$ *dB. The curve in red represents* $N = 11$ *(odd) number of elements while the curve in blue is for* $N = 10$ *(even).* **Right Plot**: *Polar plot for the parameters used on the left.*

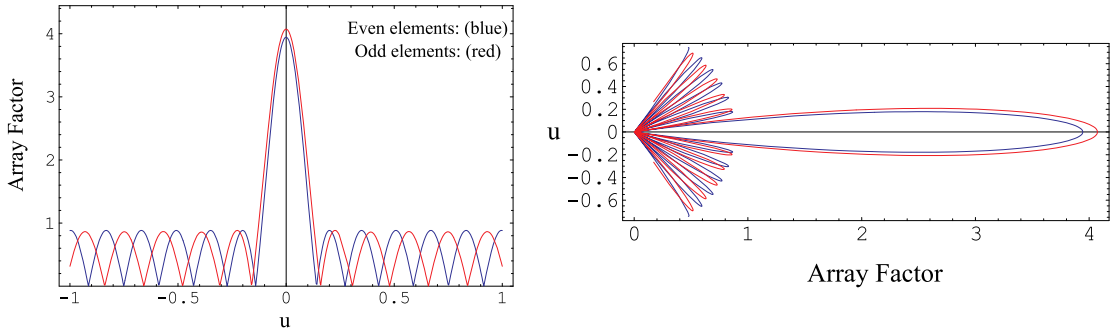

Figure 5: **Left Plot**: *The array factor as a function of* u *for* $|SLL| = -13$ *dB. The curve in red represents* $N = 17$ *(odd) number of elements while the curve in blue is for* $N = 20$ *(even).* **Right Plot**: *Polar plot for the parameters used on the left.*

Table 3: *Polynomial approximation for the $HPBW$ using the optimum spacing between the radiating elements N for a* **broadside** *array. The left hand column represents the side lobe ratio, while the right side column is the approximation to the half-power beamwidth in degrees for any $N = 3, ..., 20$.*

$\|SLL\|$ (dB)	$HPBW(degrees)$
-10	$-2.97864 \times 10^{-6}N^7 + 2.65506 \times 10^{-4}N^6 - 9.89469 \times 10^{-3}N^5$ $+0.199857N^4 - 2.3685N^3 + 16.5996N^2 - 65.1958N + 120.406$
-20	$-3.06897 \times 10^{-6}N^7 + 2.75572 \times 10^{-4}N^6 - 1.03612 \times 10^{-2}N^5$ $+0.211604N^4 - 2.54401N^3 + 18.1839N^2 - 73.4929N + 141.942$
-30	$-2.50017 \times 10^{-6}N^7 + 2.26546 \times 10^{-4}N^6 - 8.61964 \times 10^{-3}N^5$ $+0.17886N^4 - 2.19797N^3 + 16.2084N^2 - 68.618N + 142.699$
-40	$1.199797 \times 10^{-5}N^6 - 1.5909 \times 10^{-3}N^5 + 5.18349 \times 10^{-2}N^4$ $-0.889623N^3 + 8.60381N^2 - 46.0883N + 119.759$

where we define $u = \frac{\pi d}{\lambda}\cos(\theta)$, and d as being the separation between the radiating elements. The results are exact to those obtained by the MC method and are thus both displayed in Table 1. Since the variable $u \in [-1, 1]$, corresponding to $\theta = 180$ and 0 respectively, we can obtain the array factor. Generally, using this type of method, it appears that an odd number of radiating elements give a broader beamwidth, but greater 'directivity' or gain than an even number of elements. Interestingly, odd arrays can give 'better' synthesis with less number of elements but the correct choice will also depend on the requirements, eg, where the nulls appear. Figures 3-5 show the radiation pattern for different N and SLL. An interesting result arises when we consider the behaviour of large arrays as a function of the SLL. Figure 6 shows a plot of the 'average' of the radiation amplitudes $< a >$ as a function of the array elements N, for a given SLL. In particular for a -10 dB SLL[3], we can investigate the contibutions of the average of the amplitudes radiated by the array elements by the use of linear regression techniques. We define the average $< a >$ to be

$$< a >= \frac{1}{N}\sum_i a_i, \tag{36}$$

where a_i are the individual amplitudes from each of the array elements and we consider a linear fit to the data in order to obtain the expression

$$< a >= 1.00474 - 0.0406255N \tag{37}$$

where N is the number of elements for *both* the even and odd cases. Equation (37) allows us to solve for $< a >$ if the number of radiating elements are given or alternatively if $< a >$ is given, we can obtain N. Clearly the linearity of (37) is a very inaccurate approximation and a better fit to the data gives the result,

$$< a >= 1.40296 - 0.144412N + 0.00688N^2 - 0.0001223N^3. \tag{38}$$

Once again (38) allows us to solve for $< a >$ or N, however when solving (38) for N, the cubic equation can give a number of solutions, some of which will be imaginary. In order

[3]The $SLL = -10dB$ example is used here in order to demonstrate the method. The same procedure therefore applies for any SLL.

Table 4: *Polynomial approximation for the $HPBW$ using the optimum spacing between the radiating elements N for an* **endfire** *array. The left hand column represents the side lobe ratio, while the right side column is the approximation to the half-power beamwidth in degrees for any $N = 3, ..., 20$.*

$\|SLL\|$ (dB)	$HPBW(degrees)$
-10	$-2.69065 \times 10^{-6}N^7 + 2.41777 \times 10^{-4}N^6 - 9.10298 \times 10^{-3}N^5 +$ $0.186397N^4 - 2.25303N^3 + 16.3049N^2 - 68.3012N + 160.484$
-20	$-2.3982 \times 10^{-6}N^7 + 2.16965 \times 10^{-4}N^6 - 8.24329 \times 10^{-3}N^5$ $+0.170909N^4 - 2.10251N^3 + 15.613N^2 - 68.0538N + 170.946$
-30	$-1.74512 \times 10^{-6}N^7 + 1.59827 \times 10^{-4}N^6 - 6.16729 \times 10^{-3}N^5$ $+0.130493N^4 - 1.65061N^3 + 12.7594N^2 - 59.163N + 165.512$
-40	$-1.07953 \times 10^{-6}N^7 + 1.00824 \times 10^{-4}N^6 - 3.98904 \times 10^{-3}N^5$ $+8.71996 \times 10^{-2}N^4 - 1.15209N^3 + 9.45741N^2 - 47.8277N + 153.68$

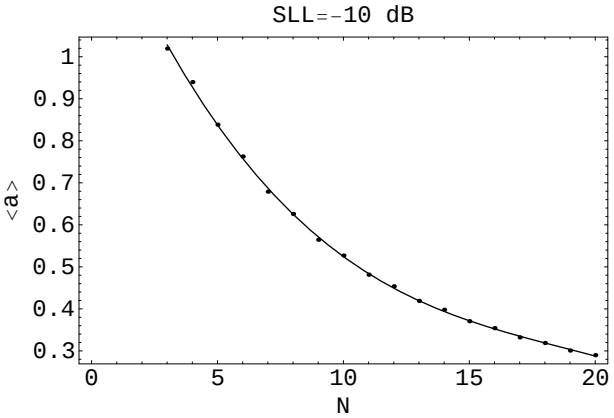

Figure 6: *The solid curve is obtained from (38), while the points represent the number of elements N for each average power $< a >$.*

to obtain the required solution, (37) is solved to obtain a value N_0, such that when solving (38) it is used as the initial guess or initial condition thereby improving considerably the accuracy of (38). We can analyse other values of the side lobe ratio in a similar way. Furthermore, the use of regression techniques means that the HPBW (in degrees) for both **broadside** and **endfire** arrays can be obtained for a given SLL if any number N for the elements is substituted. This is shown in Table 3 and Table 4 respectively.

3 The Power Aperture Product of a Weighted Array

From previous results we have seen that generally an odd number of elements, while giving a slightly broader beamwidth, has greater directivity (or gain) than an even number of elements. Interestingly, when we consider such arrays in terms of aperture power and efficiency relative to an unweighted array the opposite of what we expect occurs. For instance as we will discuss below, the optimum efficiency of the array is greatest for an *even* number of arrays even though we have a reduced gain as a result. Therefore the type of performance we require will determine the kind of trade-offs we are prepared to accept in antenna synthesis. The power aperture product of a weighted array is given by:

$$P_{array}A_{array} = \left[\sum_{i=1}^{N} \tilde{a}_{t,i}\tilde{a}_{r,i}\right]^2 P_{element}A_{element} \tag{39}$$

where we define P_{array} as the average power of the array, A_{array} as the effective area of the array, $P_{element}$ as the average power of the unweighted element (assumed identical across the array), $G_{element}$ as the gain of the unweighted element (assumed identical across the array), $\tilde{a}_{t,i}$ are the normalised amplitude weights applied on transmission to element i, $\tilde{a}_{r,i}$ are the normalised amplitude weights applied on reception to element i. Where the element normalisation is such that $max(\tilde{a}_i) = 1$, it reflects the practical issue that the antenna weighting is normally achieved by attenuating an element. For an unweighted antenna $\tilde{a}_{t,i} = 1$ and $\tilde{a}_{r,i} = 1$, reducing the previous result to the well known

$$P_{array}A_{array} = N^2 P_{element}A_{element} \tag{40}$$

The relative efficiency of the weighted antenna to the unweighted antenna is then given by:

$$\varepsilon = \frac{1}{N^2}\left[\sum_{i=1}^{N} \tilde{a}_{t,i}\tilde{a}_{r,i}\right]^2 \frac{P_{element}G_{element}}{P_{element}G_{element}} = \frac{1}{N^2}\left[\sum_{i=1}^{N} \tilde{a}_{t,i}\tilde{a}_{r,i}\right]^2 \tag{41}$$

We firstly consider the performance of arrays with Chebyshev weighting applied only once, so that *either* $\tilde{a}_{t,i} = 1$ *or* $\tilde{a}_{r,i} = 1$. Figures 7-9 show the power aperture product and the efficiency of the single weighted array for differing numbers of elements. Each of the Figures differ by the maximum number of elements shown in order to highlight the bahaviour of the arrays as the number of elements increases. What is apparent from the Figures is that for any given weighting the total power aperture product increases as the number of elements is increased, but that beyond a certain critical number of elements the power aperture rate

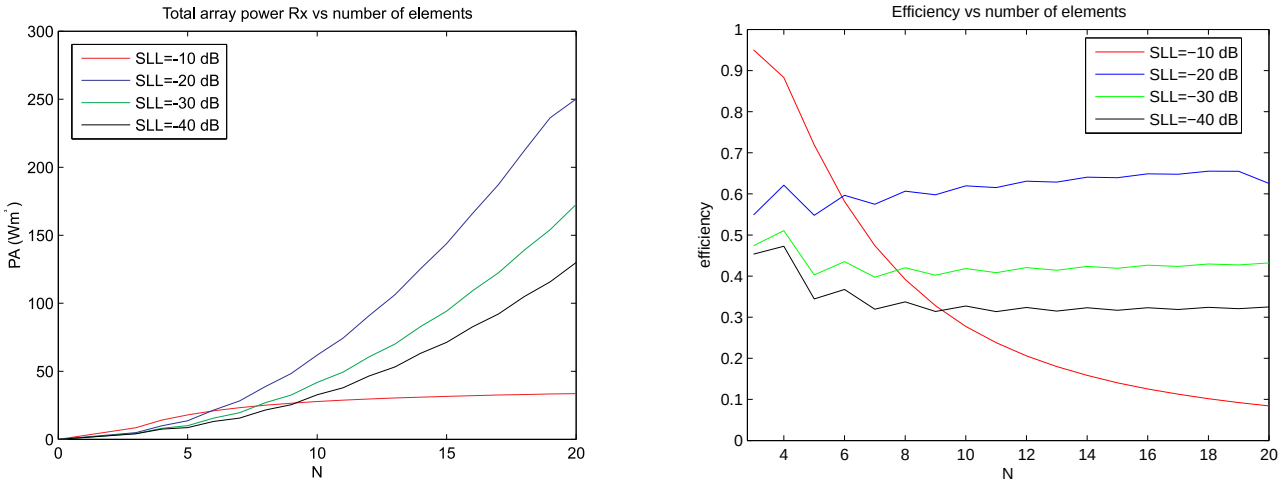

Figure 7: **Left Plot***: The total transmitted aperture power is shown vs a relatively small number of array elements N at different sidelobe levels.* **Right Plot***: The efficiency of the aperture power of arrays is shown vs the number of elements.*

of increase is sharply reduced, and the overall power aperture efficiency sharply declines. The reason for this decrease is due to the fact that the Chebyshev weights must transfer power from the main lobe to the sidelobes in order to maintain the required sidelobe ratio.

We will now consider if for a given two way side lobe level it is more efficient to weight both transmission and reception or just one (usually reception because of interference rejection considerations). Figure 10 shows the total power aperture product for two cases. In the first case, 20dB Chebyshev weighting is applied to both transmission and reception, and in the second case 40dB Chebyshev weighting is applied to the reception signal only. Figure 10 broadly shows that for small arrays it is better to apply weights on both transmission and reception, but for larger arrays it is more efficient to apply Chebyshev weights to reception only[4].

4 The Impact on the Signal to Noise Ratio of a Weighted Array

Whilst the signal levels are impacted by the weighting function applied, so are the noise levels (at least on receive), and so we must consider the overall impact on the resultant signal to noise ratio (SNR).

If we assume that the noise at each receiver is independent and of the same mean power level, then the expected value of the total noise after weighting will be:

[4]For the very smallest arrays there may be a reversal of this result, as shown in Figure 10

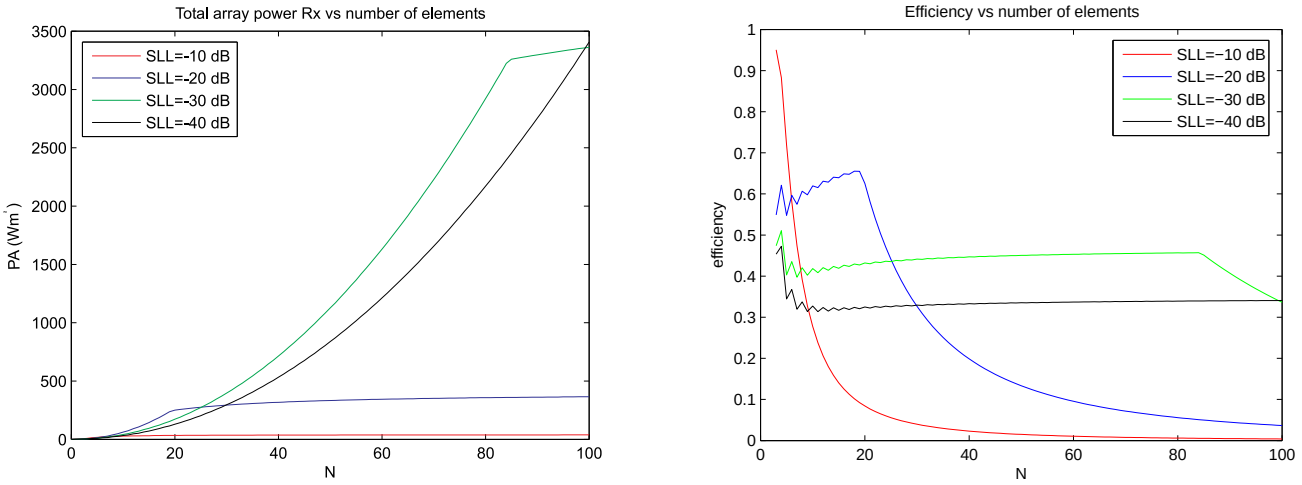

Figure 8: **Left Plot***: The total transmitted aperture power is shown vs $N = 100$ array elements at different sidelobe levels.* **Right Plot***: The efficiency of the aperture power of the arrays is shown vs the number of elements.*

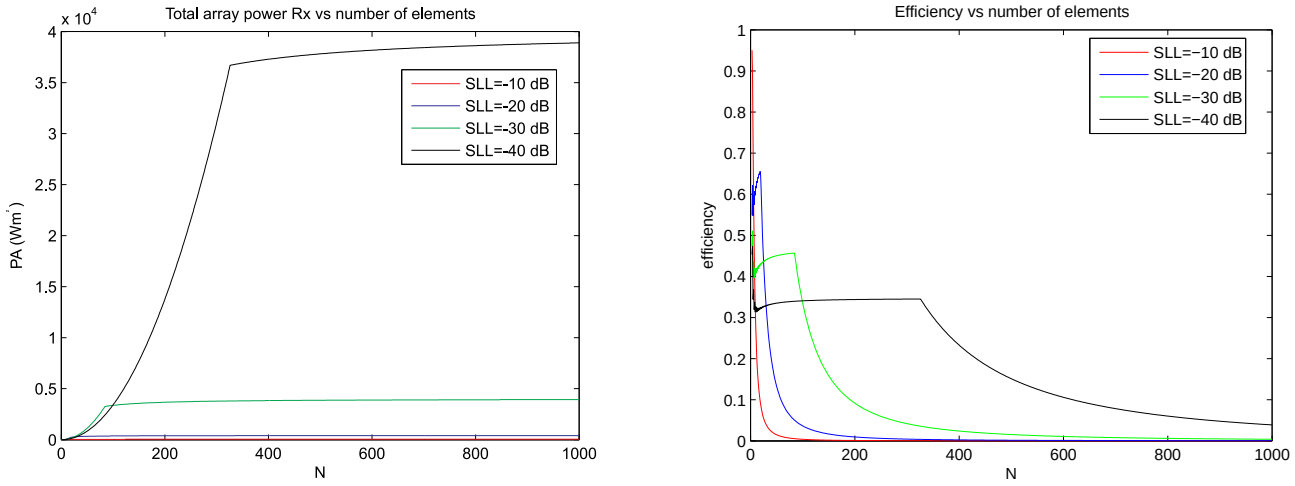

Figure 9: **Left Plot***: The total transmitted aperture power is shown vs a relatively large number of array elements at different sidelobe levels.* **Right Plot***: The efficiency of the aperture power of the arrays is shown vs the number of elements.*

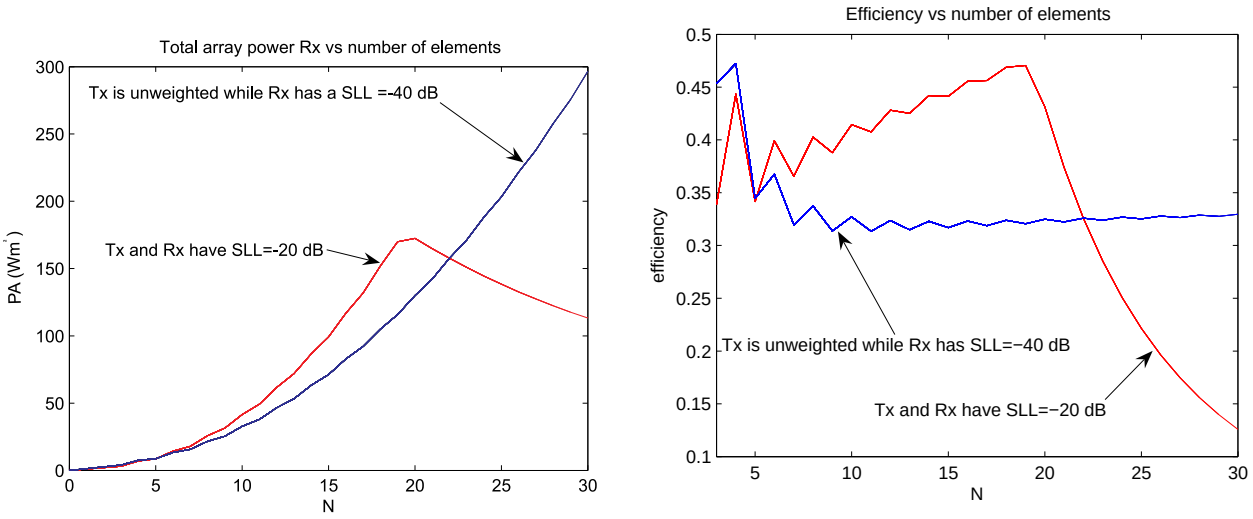

Figure 10: **Left Plot***: The total transmitted aperture power is shown vs the number of elements at different sidelobe levels for a two-way transmit and receive SLL. Comparison is made of the power for an unweighted transmition but weighted reception of SLL=-40 dB to that of a transmit and receive mode of SLL=-20 dB.* **Right Plot***: The efficiency of the aperture power of the arrays is shown vs the number of elements.*

$$n_{array} = \left[\sum_{i=1}^{N} \tilde{a}_{r,i}^2\right] n_{element} \tag{42}$$

where n_{array} is the average noise power of the array, $n_{element}$ is the average noise power of the unweighted element (assumed identical across the array), $\tilde{a}_{r,i}$ are the normalised amplitude weights applied on reception to element i. The signal to noise ratio is:

$$(SNR)_{weighted} = \frac{P_{array}}{N_{array}} = \frac{\left[\sum_{i=1}^{N} \tilde{a}_{t,i}\tilde{a}_{r,i}\right]^2}{\left[\sum_{i=1}^{N} \tilde{a}_{r,i}^2\right]} (SNR)_{element} \tag{43}$$

where

$$(SNR)_{element} = \frac{P_{element}}{n_{element}} \tag{44}$$

An array that is unweighted on both transmit and receive gives:

$$(SNR)_{un-weighted} = N(SNR)_{element} \tag{45}$$

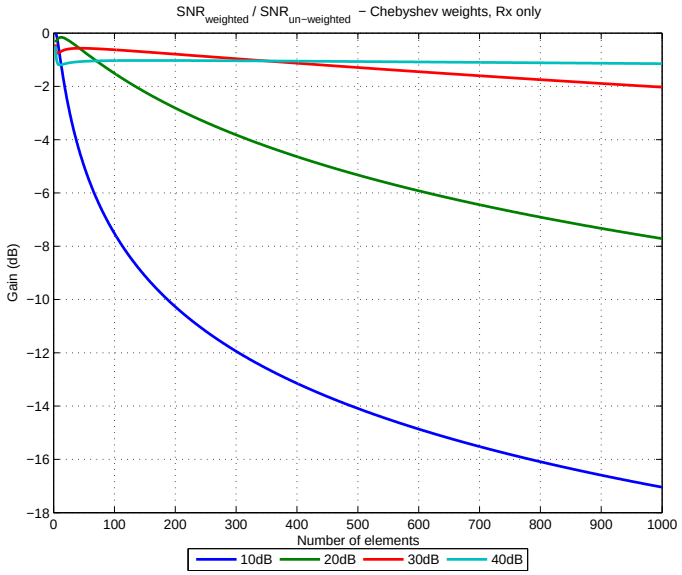

Figure 11: *Impact upon SNR of Chebyshev weights applied on reception only.*

Hence the impact upon the SNR of weighting the antenna is given by:

$$\frac{(SNR)_{weighted}}{(SNR)_{un-weighted}} = \frac{\left[\sum_{i=1}^{N} \tilde{a}_{t,i}\tilde{a}_{r,i}\right]^2}{N\left[\sum_{i=1}^{N} \tilde{a}_{r,i}^2\right]} \tag{46}$$

or

$$(SNR)_{weighted} = \frac{\left[\sum_{i=1}^{N} \tilde{a}_{t,i}\tilde{a}_{r,i}\right]^2}{N\left[\sum_{i=1}^{N} \tilde{a}_{r,i}^2\right]}(SNR)_{un-weighted} \tag{47}$$

The impact of applying Chebyschev weights only on receive (that is $\tilde{a}_{t,i} = 1$) on the system SNR is shown in Figure 11, with the loss in signal to noise again becoming significant once the natural side lobe levels are lower than the Chebyschev adjusted level. The losses shown here broadly match those reported in the literature-see for example Nathanson [7] *provided* the array is sufficiently small, otherwise the literature understates the losses that are experienced.

Using weights on both transmission and reception has a far more profound impact upon system SNR, as shown in Figure 12, with a significant loss in SNR resulting from the loss in power aperture efficiency on transmit dominating the overall SNR performance. This remains the case where the overall weighting appears nominally equal to the receive only case shown in Figure 13.

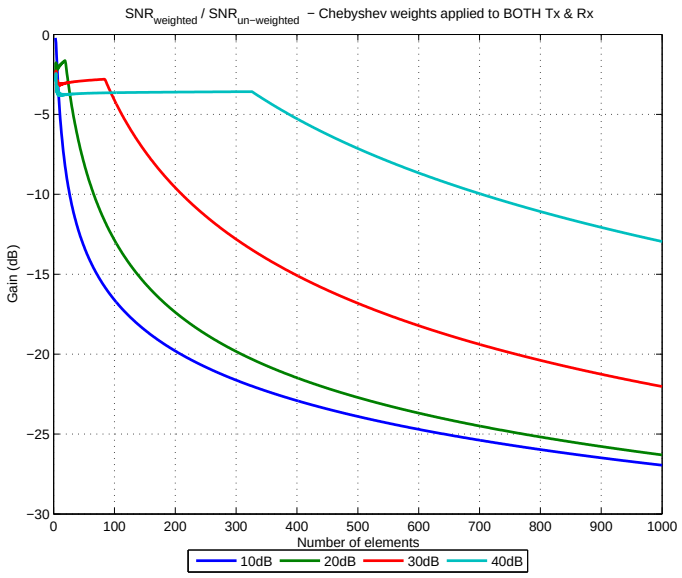

Figure 12: *Impact upon SNR of Chebyshev weights applied both on transmit and reception.*

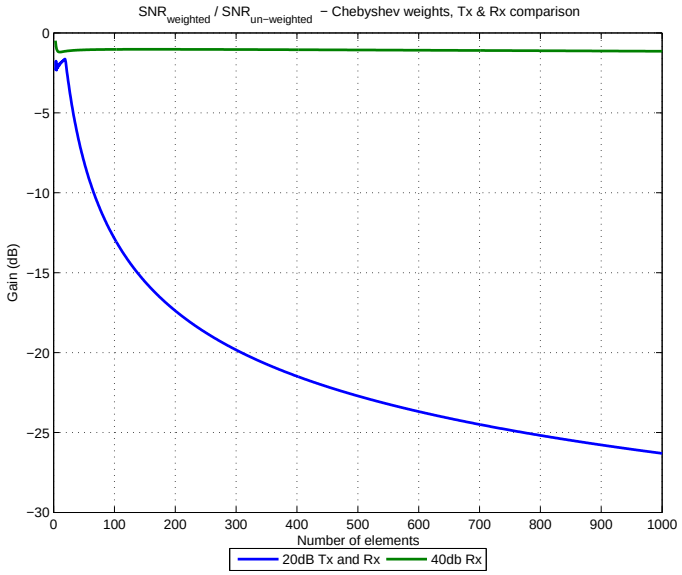

Figure 13: *Impact upon SNR of Chebyshev weights applied on transmit and reception compared with reception only.*

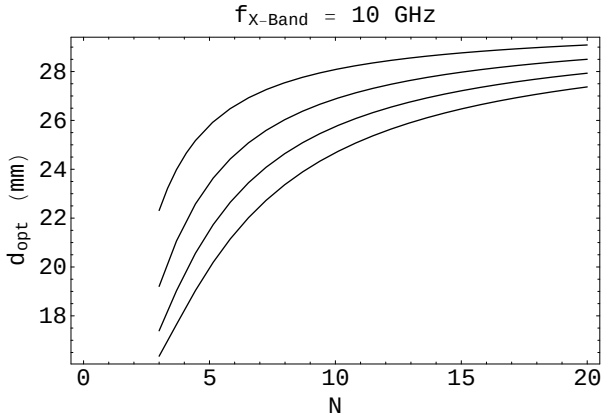

Figure 14: *The optimised spacing plotted against the number of elements for an X-Band ($\lambda = 0.03$ m) array. The curves starting from the bottom to the top correspond to $|SLL| = -10, -20, -30$ and -40 dB's respectively.*

5 Investigation of Beamwidth, Side Lobe Level and the Number of Elements

Another important parameter of interest that we will look at is the beamwidth. We consider $\theta = \theta_H$ such that it corresponds to the half-power point on the main beam of the array pattern with the appropriate phase factor α chosen according to whether we have broadside or endfire arrays. There are two half-power points for a broadside array ($\alpha = 0$), one exists on the left and the other on the right side of $\theta = \pi/2$ respectively. For the case $\theta_H < \pi/2$, the half-power beamwidth for broadside arrays is $HPBW = \pi - 2\theta_H$. On the other hand, for endfire arrays ($\alpha = \pm\beta d$), there exists only one solution for θ_H so that $HPBW = \theta_H$ when $\alpha = -\beta d$ and $HPBW = \pi - \theta$ when $\alpha = +\beta d$. Here we will consider $\alpha = -\beta d$ for the endfire case without loss of generality [3], and note that for $d = \lambda/2$, $\theta_H = HPBW/2$. We define $\psi = \psi_H$ at $\theta = \theta_H$, so that for the broadside case $\psi_H = \beta d \cos(\theta_H)$, and for the endfire case $\psi_H = \beta d\,[\cos(\theta_H) - 1]$. From (3) we have

$$\bar{\psi}_H = 2\cosh^{-1}\left[\gamma \cos\left(\frac{\psi_H}{2}\right)\right]. \tag{48}$$

We recall that the array factor assumes its maximum value at $\bar{\psi} = \bar{\psi}_0$, so that from equations (3), (5) and (6) after combining we obtain

$$\cos\left(\frac{\psi_H}{2}\right)\cosh\left[\frac{1}{N-1}\cosh^{-1}(R)\right] - \cosh\left[\frac{1}{N-1}\cosh^{-1}(\frac{\sqrt{2}}{2}R)\right] = 0. \tag{49}$$

Equation (49) gives the relationship between the half-power beamwidth, side lobe level and the number of elements. More specifically if two of these are given, the third one can be calculated. Thus, for the case where N and $HPBW$ are given, we can determine R. As can be seen from (49) however, the equation involves transcendental functions and so the solution for R needs to be found numerically. Any number of solutions can satisfy (49) so that in order to pick the correct solution we must firstly guess a 'root' as an initial

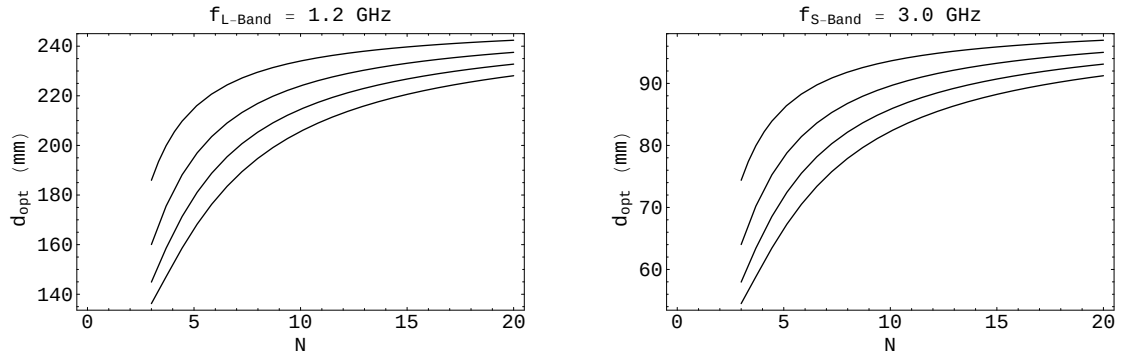

Figure 15: *The optimised spacing plotted against the number of elements for an L-Band ($\lambda = 0.25$ m) array on the left and an S-Band ($\lambda = 0.1$ m) array on the right. The curves starting from the bottom to the top correspond to $|SLL| = -10, -20, -30$ and -40 dB's respectively.*

condition before proceeding. This means that (49) needs to be used with caution. For example, if we want to find the number of elements N for a given R and $HPBW$, we find that N is a non-integer number which physically is impractical. The correct solution would be

$$N = \text{int}\,\{N_0\} + 1, \tag{50}$$

where int $\{N_0\}$ means the integer part of the solution N_0 obtained numerically from (49). To further highlight the method, we consider an endfire array with $|SLL| = -20$ dB and a half-power beamwidth of 22.5^0. By the use of (49) we find the numerical solution to be $N_0 = 13.596$ but because of (50) and the fact that we need to have $HPBW \leq 22.50^0$, the actual solution is $N = 14$. The beamwidth is obtained from

$$HPBW = \pi - 2\cos^{-1}\left(\frac{\psi_H}{\beta d}\right) \qquad \text{for} \quad \text{broadside} \tag{51}$$

and

$$HPBW = \cos^{-1}\left(1 - \frac{\psi_H}{\beta d}\right) \qquad \text{for} \quad \text{end} - \text{fire}, \tag{52}$$

where from (49) we transpose to get

$$\psi_H = 2\cos^{-1}\left\{\frac{\cosh\left[\frac{1}{N-1}\cosh^{-1}(\frac{R}{\sqrt{2}})\right]}{\cosh\left[\frac{1}{N-1}\cosh^{-1}(R)\right]}\right\}. \tag{53}$$

For endfire arrays where the inter-element spacing is $d = \lambda/2$, we multiply the right-hand side of (52) by the factor 2. Figures 14-15 show results for frequency bands of interest.
For selected SLL, the optimum configuration is obtained by the given optimum element separation and number of elements. In fact all variables can be calculated simultaneously by looking at the graphs, ie, if we require the optimum performance for the array then for a selected optimum element separation we read off the corresponding number of elements and SLL and so on. Similarly, the variation of the HPBW (in degrees) as obtained for optimum element separation and $\lambda/2$ separation for both *broadside* and *endfire* arrays is shown in Figures 16-20.

6 Optimising the Inter-Element Separation

We are interested in obtaining the distance between the elements, d, such that for a specified SLL and given number of elements the smallest beamwidth can be achieved. This means 'packing' as many side lobes as possible within the radiation pattern of the array. In fact by doing so, the visible range in the $\bar{\psi}$ domain, which corresponds to the range $0 \leq \theta \geq \pi$, is determined in such a way as to include all side lobes on both sides of the main beam for broadside arrays and on one side of it for endfire arrays. A portion of the grating lobe which will produce a side lobe with a magnitude equal to the specified SLL is also included. The cutoff point on the grating lobe satisfies the relation [3]:

$$\cosh\left[\frac{(N-1)}{2}\bar{\psi}\right] = \left|\cos\left[\frac{(N-1)}{2}\bar{\psi}\right]\right|, \tag{54}$$

that is valid only if $\bar{\psi} = 0$. The solution of ψ which corresponds to the grating lobe lies in the range $\pi < \psi < 2\pi$. In this range however, $\cos(\psi/2) < 0$ and (4) should be modified as $-\gamma\cos(\psi/2) = \cos(\bar{\psi}/2)$. If we put $\bar{\psi} = 0$ in the previous expression we obtain $\psi = 2\pi - 2\cos^{-1}(1/\gamma)$. For broadside arrays, ψ should correspond to $\theta = 0$, that is when $\psi = \beta d_{opt}$, where d_{opt} is the optimum spacing between the elements. As a result we have

$$d_{opt} = \lambda\left[1 - \frac{\cos^{-1}(\frac{1}{\gamma})}{\pi}\right] \qquad broadside. \tag{55}$$

In the case of endfire arrays with the main beam in the $\theta = \pi$ direction, ψ should correspond to $\theta = 0$, in other words $\psi = 2\beta d_{opt}$, resulting in

$$d_{opt} = \frac{\lambda}{2}\left[1 - \frac{\cos^{-1}(\frac{1}{\gamma})}{\pi}\right] \quad end-fire. \tag{56}$$

Equation (56) is also valid for endfire arrays with the main beam in the $\theta = 0$, $(\alpha = -\beta d)$, direction. Optimisation of the element spacing d for endfire arrays has also been studied for the case $\alpha \neq \pm\beta d$, see [6].

7 Directivity

In this section we will consider the directivity of arrays with arbitrary spacing between the radiating elements. Stegen [7] has investigated the case when the elements have a spacing that is an integer multiple of half a wavelength. Approximations have also been obtained for the directivity of a large number of elements [8]. The more interesting case of an analytical representation for the directivity in the general case of arbitrary element spacing and arbitrary number of elements is very useful [9]. In what follows, we will obtain the results that allow us to calculate the directivity of arrays as a function of the number of elements, element spacing, and side lobe level. The results are particularly useful when the number of elements are not large and the element spacing is not an integer multiple of half a wavelength. We begin by recalling the form of the array factor for a Chebyshev array which consists of N equally spaced isotropic elements,

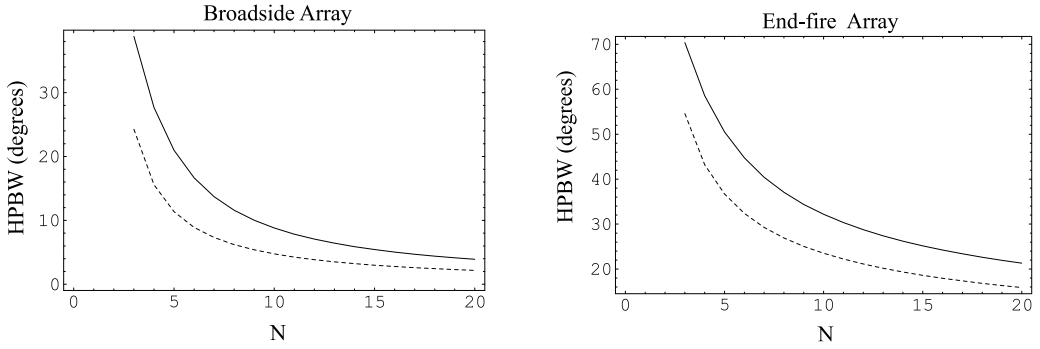

Figure 16: *Comparison of the half-power beamwidth (HPBW) for a broadside array (left) and an endfire array (right) with optimum spacing between the elements. The dashed curve's side lobe ratio is -10 dB, while the solid curve is that for a -40 dB side lobe ratio.*

$$f(\psi) = \frac{1}{R}\cos\left[(N-1)\cos^{-1}(\gamma\cos\left(\frac{\psi}{2}\right))\right], \tag{57}$$

when $|f(\psi)| \leq 1/R$, and

$$f(\psi) = \frac{1}{R}\cosh\left[(N-1)\cosh^{-1}(\gamma\cos\left(\frac{\psi}{2}\right))\right], \tag{58}$$

when $|f(\psi)| \geq 1/R$. As before, $\psi = \beta d\cos\theta + \alpha$, d is the element spacing, α is the inter-element phase shift, $\beta = 2\pi/\lambda$, λ is the wavelength and θ is the angle measured from the line that is perpendicular to the array. Here R is the beam maximum to side lobe level ratio and $\gamma = \cosh\left[\ln(R+\sqrt{R^2-1})/(N-1)\right]$. The expression for the directivity can be obtained from many publications, for example see [10], and is generally denoted as:

$$\begin{aligned} D &= \frac{4\pi}{\int_0^{\pi}\int_0^{2\pi} f^2(\theta)\sin(\theta)d\theta d\phi} \\ &= \frac{4\pi d/\lambda}{\int_{\alpha-\beta d}^{\alpha+\beta d} f^2(\psi)d\psi}. \end{aligned} \tag{59}$$

In order to evaluate the integral in the denominator of (59), we notice that the expression $f(\psi)$ as given by (57) or (58) can be expanded as a series in $\cos(nx)$ or $\cosh(nx)$ respectively. By collecting terms we arrive at the result for $f^2(\psi)$:

$$f^2(\psi) = \frac{1}{4R^2}\left[2 + \chi_0^{2M} + 2M\sum_{i=1}^{M}(-1)^i\left(\frac{1}{i}\right)\begin{pmatrix} 2M-i-1 \\ i-1 \end{pmatrix}\chi_0^{2(M-i)}\right], \tag{60}$$

where $M = N-1$ and $\chi_0 = 2\gamma\cos(\psi/2)$. By substituting (60) into (59) and using the identity,

$$\int\cos^{2n}(x)dx = 2^{-2n}\begin{pmatrix} 2n \\ n \end{pmatrix}x + 2^{1-2n}\sum_{k=0}^{n-1}\begin{pmatrix} 2n \\ k \end{pmatrix}\frac{\sin\left[(2n-2k)x\right]}{(2n-2k)} \tag{61}$$

we obtain the directivity D as

$$D = \frac{4R^2}{\tau} \tag{62}$$

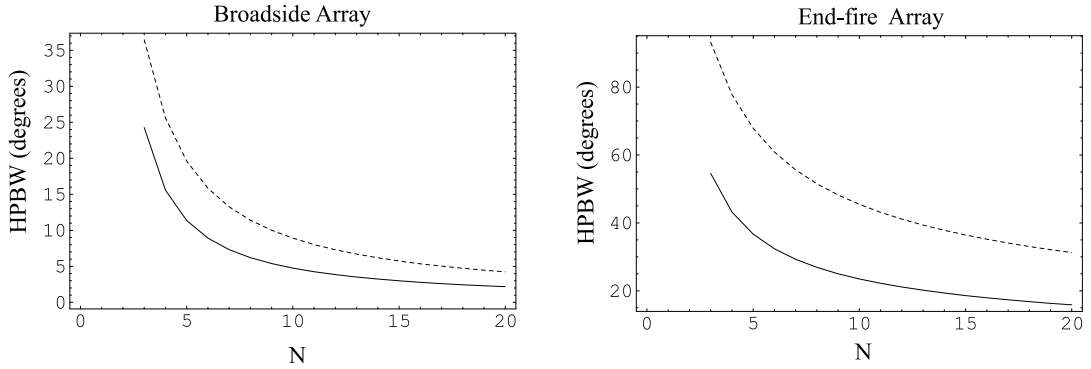

Figure 17: *The half-power beamwidth ($HPBW$) in degrees plotted against the number of elements for a broadside array (left) and an endfire array (right). The dashed curve represents an array spacing of $\lambda/2$ while the solid curve is the optimised spacing. The magnitude of the side lobe level is -10 dB.*

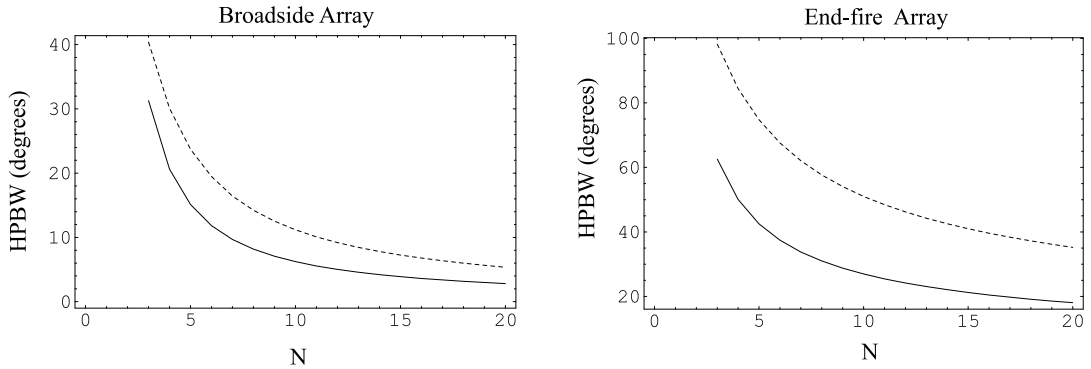

Figure 18: *The half-power beamwidth ($HPBW$) in degrees plotted against the number of elements for a broadside array (left) and an endfire array (right). The dashed curve represents an array spacing of $\lambda/2$ while the solid curve is the optimised spacing. The magnitude of the side lobe level is -20 dB.*

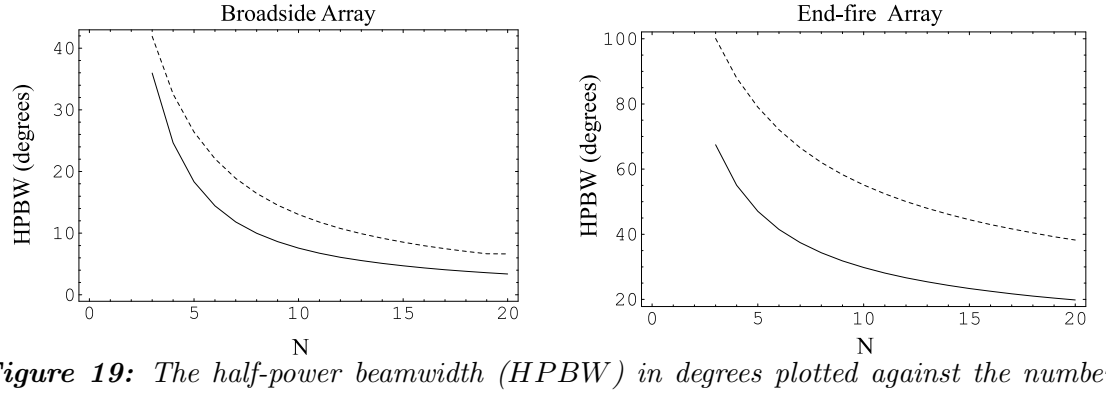

Figure 19: *The half-power beamwidth ($HPBW$) in degrees plotted against the number of elements for a broadside array (left) and an endfire array (right). The dashed curve represents an array spacing of $\lambda/2$ while the solid curve is the optimised spacing. The magnitude of the side lobe level is -30 dB.*

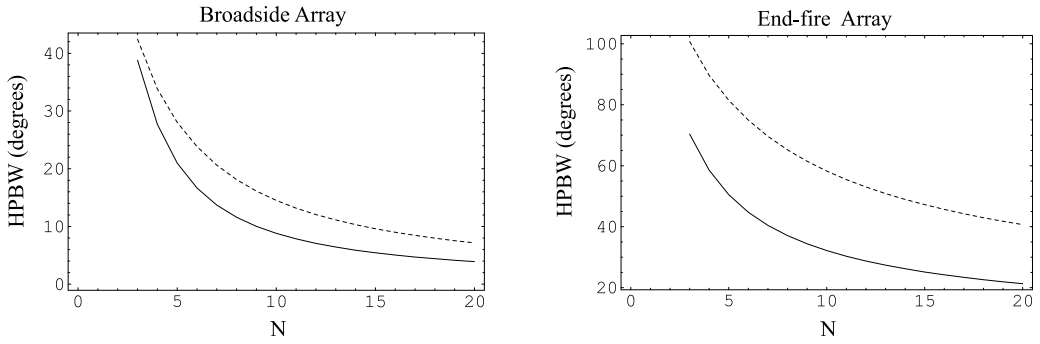

Figure 20: *The half-power beamwidth (HPBW) in degrees plotted against the number of elements for a broadside array (left) and an end-fire array (right). The dashed curve represents an array spacing of $\lambda/2$ while the solid curve is the optimised spacing. The magnitude of the side lobe level is -40 dB.*

where

$$\tau = 2 + h(0) + 2M \sum_{i=1}^{M} (-1)^i \left(\frac{1}{i}\right) \left(\begin{array}{c} 2M-i-1 \\ i-1 \end{array} \right) h(i) \tag{63}$$

and

$$h(i) = \gamma^{2(M-i)} \left[\left(\begin{array}{c} 2M-2i \\ M-i \end{array} \right) + 2 \sum_{k=0}^{M-i-1} \left(\begin{array}{c} 2M-2i \\ k \end{array} \right) \zeta(i,k) \right] \tag{64}$$

while

$$\zeta(i,k) = \frac{1}{\beta d} \frac{\sin\left[(M-i-k)\beta d\right] \cos\left[(M-i-k)\alpha\right]}{(M-i-k)}. \tag{65}$$

Equation (64) can be simplified further if we consider a broadside array ($\alpha = 0$) or endfire array ($\alpha = \pm\beta d$) so that for both of these cases we have

$$\zeta(i,k) = \frac{\sin\left[\nu(M-i-k)\beta d\right]}{\nu\beta d(M-i-k)}, \tag{66}$$

where

$$\begin{array}{ll} \nu = 1 & broadside \\ \nu = 2 & end-fire. \end{array} \tag{67}$$

Calculations show that for the same number of elements and side lobe level, the directivity of a broadside array with arbitrary element spacing d, is related to the directivity of an endfire array with an element spacing of $d/2$, ie, (see Fig 21)

$$D_{broadside}(d) = D_{end-fire}(d/2). \tag{68}$$

Furthermore, when d is a multiple integer of $\lambda/2$ and $\beta d = m\pi$, where m is an integer, we find that $\zeta(i,k) = 0$. For this latter case, τ in (62) becomes:

$$\tau = 2 + \gamma^{2M} \left[\left(\begin{array}{c} 2M \\ M \end{array} \right) + 2M \sum_{i=1}^{M} (-1)^i \left(\frac{\gamma^{-2i}}{i}\right) \left(\begin{array}{c} 2M-i-1 \\ i-1 \end{array} \right) \left(\begin{array}{c} 2M-2i \\ M-i \end{array} \right) \right]. \tag{69}$$

Thus we find that when $d = \lambda/2$, the directivity of broadside and endfire arrays is

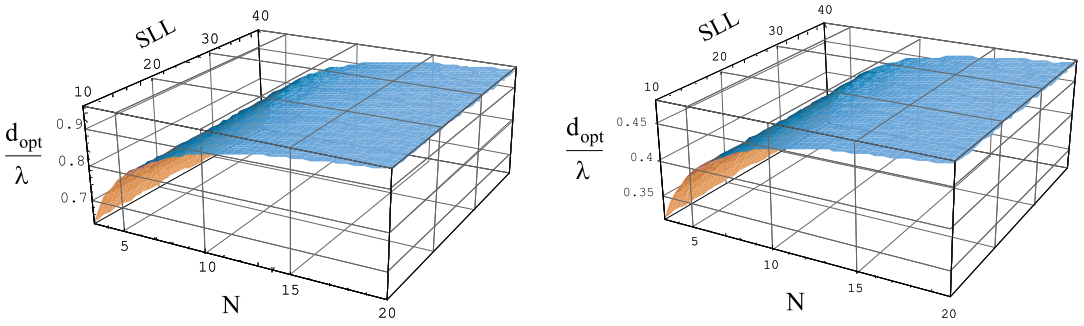

Figure 21: *The relation between the SLL, the ratio of the optimum spacing to the wavelength (d_{opt}/λ) and the number of elements N. The plot on the left is for a* **broadside** *array while the plot on the right is for an* **endfire** *array.*

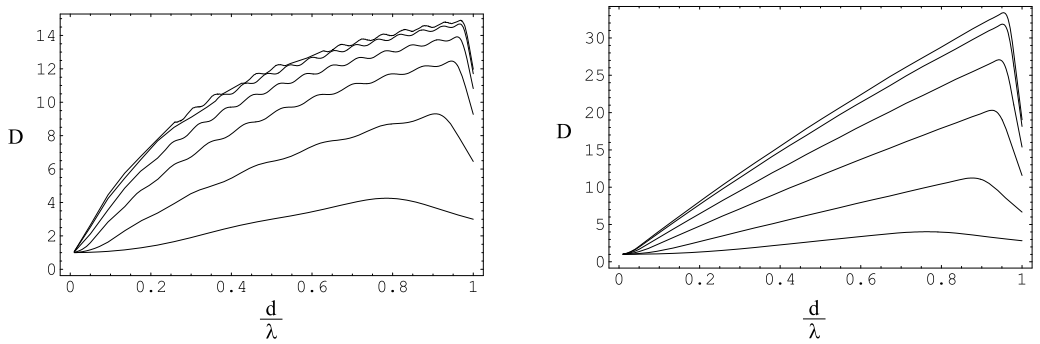

Figure 22: *Plots of the directivity D against the ratio d/λ for a broadside array (the endfire case differs by a factor of 1/2). The number of elements that have been chosen are $N = 3, 7, 12, 16, 19$ and 20, where $N = 3$ is the lowest curve and $N = 20$ is the highest in each plot. The side lobe level is:* **-10 dB for the left plot and -20 dB for the right plot**.

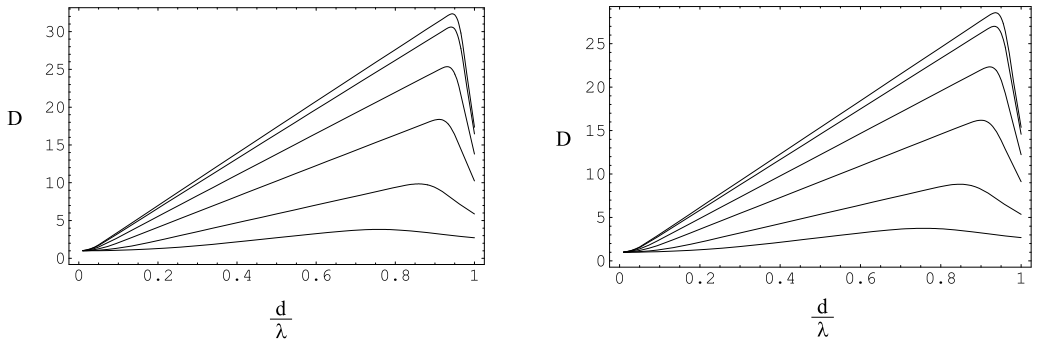

Figure 23: *Plots of the directivity D against the ratio d/λ for a broadside array (the endfire case differs by a factor of 1/2). The number of elements that have been chosen are $N = 3, 7, 12, 16, 19$ and 20, where $N = 3$ is the lowest curve and $N = 20$ is the highest in each plot. The side lobe level is:* **-30 dB for the left plot and -40 dB for the right plot**.

equivalent. For a specified number of elements N, side lobe level and element spacing d/λ, we can apply (62)-(65) to calculate the directivity. On the other hand if d is a integer multiple of $\lambda/2$, we can use the expression for τ as given by (69). Figures (22-23) show plots of the directivity against the ratio d/λ for broadside arrays with the endfire curves differing only by a factor of $1/2$. From the graphs we can see that the curves 'peak' for given values of the ratio d/λ. The element spacing d (in d/λ) corresponding to the maximum of the directivity is not equal to the optimum spacing, ie, $d \neq d_{opt}$. In other words, we find that minimum beamwidth and maximum directivity do not occur simultaneously. The results presented here are very useful when we are dealing with situations where the element spacing is different from integral multiples of half a wavelength and the number of elements is not too large.

8 Conclusion

We have studied arrays based on a modification of conventional Chebyshev arrays. Chebyshev arrays have the property that the side lobe levels are the same but are hindered by the fact that the directivity 'saturates', especially as the number of elements increases. The MC method also has the same side lobe levels but the directivity is vastly improved even when using the same parameters as for the conventional Chebyshev method. The higher directivity in the MC method is achieved by finding the zeros of conventional Chebyshev arrays repeatedly. However the maximum directivity is achieved when the spacing between the elements is slightly smaller than the optimum element spacing in the case of the MC method. The 3 dB beamwidth narrows or broadens depending on the number of elements chosen with pronounced differences if even or odd elements are chosen. All parameters for such arrays have been studied and comparisons have also been made between *broadside* and $endfire$ arrays.

Acknowledgment

The author would like to thank Dr Andrew Shaw and Dr Brett Haywood for helpful comments and suggestions.

References

1. R.J. Mailloux, *Phased array antenna handbook*, Artech House, Boston, (1994).

2. T.T. Taylor, *Design of line source antennas for narrow beamwidth and low side lobe*, IEEE Trans., **AP − 3**, pp. 16-28, (1955).

3. A. Safaai-Jazi, IEEE Trans., **AP − 42**(3), pp. 439-443, (1994).

4. K.F. Lee, *Principles of Antenna Theory*, New York, John Wiley and Sons, Chapter. 7, (1984).

5. D. Barbiere, Proc. IRE, Jan issue, pp. 78-82, (1952).

6. R.C. Johnson and H. Jasik, *Antenna Engineering Handbook*, New York, McGraw-Hill, Chapter 3, (1984).

7. F.E. Nathanson, *Radar Design Principles-2nd Edition*.

8. R.J. Stegen, IRE Trans., **AP − 8**, pp 629-631, (1960).

9. R.S. Elliot, *The theory of antenna arrays*, Chapter 1 of R.C. Hansen (ed):*Microwave scanning antennas*, Academic Press, New York, (1966).

10. A. Safaai-Jazi, Electron. Lett., **31** (10), pp. 772-774, (1995).

11. W.L. Stutzman and G.A. Thiele, *Antenna theory and design*, Wiley, New York, (1981).

DISTRIBUTION LIST

Phased Array Analysis Using a Modified Chebyshev Approach

Dr Aris Alexopoulos

AUSTRALIA

DEFENCE ORGANISATION	**No. of copies**
Task Sponsor	
DGMD	1 Printed
S&T Program	
Chief Defence Scientist	1
Deputy Chief Defence Scientist Policy	1
AS Science Corporate Management	1
Director General Science Policy Development	1
Counsellor Defence Science, London	Doc Data Sheet
Counsellor Defence Science, Washington	Doc Data Sheet
Scientific Adviser to MRDC, Thailand	Doc Data Sheet
Scientific Adviser Joint	1
Navy Scientific Adviser	1
Scientific Adviser – Army	1
Air Force Scientific Adviser	1
Scientific Adviser to the DMO	1
Systems Sciences Laboratory	
Chief of Electronic Warfare and Radar Division: Dr Len Sciacca	Doc Data Sheet
Research Leader of Microwave Radar Branch: Dr Andrew Shaw	1 Printed
Head of Radar Modelling and Analysis Group: Dr Brett Haywood	1 Printed
Author: Dr Aris Alexopoulos, EWRD	20 Printed
Dr Graham V. Weinberg, EWRD	1 Printed
DSTO Library and Archives	
Library Fishermans Bend	Doc Data Sheet
Library Edinburgh	2 Printed
Defence Archives	1 Printed
Library, Sydney	Doc Data Sheet
Library, Stirling	Doc Data Sheet
Library Canberra	Doc Data Sheet
Capability Development Group	
Director General Maritime Development	Doc Data Sheet
Director General Land Development	1
Director General Capability and Plans	Doc Data Sheet
Assistant Secretary Investment Analysis	Doc Data Sheet

Director Capability Plans and Programming	Doc Data Sheet
Chief Information Officer Group	
Director General Australian Defence Simulation Office	Doc Data Sheet
AS Information Strategy and Futures	Doc Data Sheet
Director General Information Services	Doc Data Sheet
Strategy Group	
Director General Military Strategy	Doc Data Sheet
Assistant Secretary Governance and Counter-Proliferation	Doc Data Sheet
Navy	
Maritime Operational Analysis Centre, Building 89/90 Garden Island Sydney NSW Deputy Director (Operations) Deputy Director (Analysis)	Doc Data Sht & Dist List
Director General Navy Capability, Performance and Plans, Navy Headquarters	Doc Data Sheet
Director General Navy Strategic Policy and Futures, Navy Headquarters	Doc Data Sheet
Air Force	
SO (Science) - Headquarters Air Combat Group, RAAF Base, Williamtown NSW 2314	Doc Data Sht & Exec Summ
Army	
ABCA National Standardisation Officer Land Warfare Development Sector, Puckapunyal	e-mailed Doc Data Sheet
SO (Science) - Land Headquarters (LHQ), Victoria Barracks NSW	Doc Data & Exec Summary
SO (Science), Deployable Joint Force Headquarters (DJFHQ) (L), Enoggera QLD	Doc Data Sheet
Joint Operations Command	
Director General Joint Operations	Doc Data Sheet
Chief of Staff Headquarters Joint Operations Command	Doc Data Sheet
Commandant ADF Warfare Centre	Doc Data Sheet
Director General Strategic Logistics	Doc Data Sheet
COS Australian Defence College	Doc Data Sheet
Intelligence and Security Group	
AS Concepts, Capability and Resources	1
DGSTA , Defence Intelligence Organisation	1 Printed
Manager, Information Centre, Defence Intelligence Organisation	1
Director Advanced Capabilities	Doc Data Sheet
Defence Materiel Organisation	
Deputy CEO	Doc Data Sheet
Head Aerospace Systems Division	Doc Data Sheet
Head Maritime Systems Division	Doc Data Sheet
Program Manager Air Warfare Destroyer	Doc Data Sheet
CDR Joint Logistics Command	

Guided Weapon & Explosive Ordnance Branch (GWEO)	Doc Data Sheet

OTHER ORGANISATIONS

National Library of Australia	1
NASA (Canberra)	1

UNIVERSITIES AND COLLEGES

Australian Defence Force Academy

Library	1
Head of Aerospace and Mechanical Engineering	1
Hargrave Library, Monash University	Doc Data Sheet

OUTSIDE AUSTRALIA

INTERNATIONAL DEFENCE INFORMATION CENTRES

US Defense Technical Information Center	1
UK Dstl Knowledge Services	1
Canada Defence Research Directorate R&D Knowledge & Information Management (DRDKIM)	1
NZ Defence Information Centre	1

ABSTRACTING AND INFORMATION ORGANISATIONS

Library, Chemical Abstracts Reference Service	1
Engineering Societies Library, US	1
Materials Information, Cambridge Scientific Abstracts, US	1
Documents Librarian, The Center for Research Libraries, US	1

SPARES

DSTO Edinburgh Research Library	5 Printed

Total number of copies: 57 Printed: 33 PDF: 24

DEFENCE SCIENCE AND TECHNOLOGY ORGANISATION DOCUMENT CONTROL DATA				1. CAVEAT/PRIVACY MARKING
2. TITLE Phased Array Analysis Using a Modified Chebyshev Approach			3. SECURITY CLASSIFICATION Document (U) Title (U) Abstract (U)	
4. AUTHOR Aris Alexopoulos			5. CORPORATE AUTHOR Defence Science and Technology Organisation PO Box 1500 Edinburgh, South Australia 5111, Australia	
6a. DSTO NUMBER DSTO–TR–1806	6b. AR NUMBER AR-013-548		6c. TYPE OF REPORT Technical Report	7. DOCUMENT DATE November, 2005
8. FILE NUMBER 2004/1073118/1	9. TASK NUMBER NAV 01/299	10. SPONSOR DGMD	11. No OF PAGES 29	12. No OF REFS 11
13. URL OF ELECTRONIC VERSION http://www.dsto.defence.gov.au/corporate/reports/DSTO–TR–1806.pdf			14. RELEASE AUTHORITY Chief, Electronic Warfare and Radar Division	
15. SECONDARY RELEASE STATEMENT OF THIS DOCUMENT *Approved For Public Release* OVERSEAS ENQUIRIES OUTSIDE STATED LIMITATIONS SHOULD BE REFERRED THROUGH DOCUMENT EXCHANGE, PO BOX 1500, EDINBURGH, SOUTH AUSTRALIA 5111				
16. DELIBERATE ANNOUNCEMENT No Limitations				
17. CITATION IN OTHER DOCUMENTS No Limitations				
18. DSTO RESEARCH LIBRARY THESAURUS Phased Array Radar, Chebyshev Analysis, Array Synthesis				

19. ABSTRACT

This report studies the antenna synthesis characteristics of linear phased arrays for both the *broadside* and *endfire* cases. The underlying technique is based on a modification of the conventional Dolph-Chebyshev side lobe tapering technique. Some of the parameters that are paramount in the design of these arrays are analysed, such as the number of elements N, the phase factor, side lobe levels, directivity, radiation pattern, element separation and impact upon SNR. The results are compared and the optimised configuration is investigated for each case.